Nanodroplet real-time PCR system with laser assisted heating

Hanyoup Kim,[1] Sanhita Dixit,[1] Christopher J. Green,[2] and Gregory W. Faris[1,*]

[1]Molecular Physics Laboratory and [2]Biosciences Division, SRI International, 333 Ravenswood Avenue, Menlo Park, California 94025, USA

[*]Corresponding author: gregory.faris@sri.com

Abstract: We report the successful application of low-power (~30 mW) laser radiation as an optical heating source for high-speed real-time polymerase chain reaction (PCR) amplification of DNA in nanoliter droplets dispersed in an oil phase. Light provides the heating, temperature measurement, and Taqman real-time readout in nanoliter droplets on a disposable plastic substrate. A selective heating scheme using an infrared laser appears ideal for driving PCR because it heats only the droplet, not the oil or plastic substrate, providing fast heating and completing the 40 cycles of PCR in 370 seconds. No microheaters or microfluidic circuitry were deposited on the substrate, and PCR was performed in one droplet without affecting neighboring droplets. The assay performance was quantitative and its amplification efficiency was comparable to that of a commercial instrument.

OCIS codes: (170.0170) Medical optics and biotechnology; (170.2520) Fluorescence microscopy; (170.3890) Medical optics instrumentation

References and links

1. G. L. Liu, J. Kim, Y. Lu, and L. P. Lee, "Optofluidic control using photothermal nanoparticles," Nature Mater. **5**, 27-32 (2006).
2. C. N. Baroud, J. P. Delville, F. Gallaire, and R. Wunenburger, "Thermocapillary valve for droplet production and sorting," Phys. Rev. E **75**, 046302 (2007).
3. K. T. Kotz, K. A. Noble, and G. W. Faris, "Optical microfluidics," Appl. Phys. Lett. **85**, 2658-2660 (2004).
4. S. Rybalko, N. Magome, and K. Yoshikawa, "Forward and backward laser-guided motion of an oil droplet," Phys. Rev. E **70**, 046301 (2004).
5. A. D. Griffiths and D. S. Tawfik, "Miniaturising the laboratory in emulsion droplets," Trends Biotech. **24**, 395-402 (2006).
6. S. Haeberle and R. Zengerle, "Microfluidic platforms for lab-on-a-chip applications," Lab Chip **7**, 1094-1110 (2007).
7. S. Y. Teh, R. Lin, L. H. Hung, and A. P. Lee, "Droplet microfluidics," Lab Chip **8**, 198-220 (2008).
8. K. T. Kotz, Y. Gu, and G. W. Faris, "Optically addressed droplet-based protein assay," J. Am. Chem. Soc. **127**, 5736-5737 (2005).
9. C. N. Baroud, M. R. de Saint Vincent, and J. P. Delville, "An optical toolbox for total control of droplet microfluidics," Lab Chip **7**, 1029-1033 (2007).
10. N. R. Beer, B. J. Hindson, E. K. Wheeler, S. B. Hall, K. A. Rose, I. M. Kennedy, and B. W. Colston, "On-chip, real-time, single-copy polymerase chain reaction in picoliter droplets," Anal. Chem. **79**, 8471-8475 (2007).
11. K. D. Dorfman, M. Chabert, J. H. Codarbox, G. Rousseau, P. de Cremoux, and J. L. Viovy, "Contamination-free continuous flow microfluidic polymerase chain reaction for quantitative and clinical applications," Anal. Chem. **77**, 3700-3704 (2005).
12. Z. Guttenberg, H. Müller, H. Habermüller, A. Geisbauer, J. Pipper, J. Felbel, M. Kielpinski, J. Scriba, and A. Wixforth, "Planar chip device for PCR and hybridization with surface acoustic wave pump," Lab Chip **5**, 308-317 (2005).
13. P. Neuzil, C. Zhang, J. Pipper, S. Oh, and L. Zhuo, "Ultra fast miniaturized real-time PCR: 40 cycles in less than six minutes," Nucleic Acids Res. **34**, e77 (2006).
14. K. Sun, A. Yamaguchi, Y. Ishida, S. Matsuo, and H. Misawa, "A heater-integrated transparent microchannel chip for continuous-flow PCR," Sens. Actuators B **84**, 283-289 (2002).

#103676 - $15.00 USD Received 11 Nov 2008; revised 18 Dec 2008; accepted 20 Dec 2008; published 24 Dec 2008

15. B. C. Giordano, J. Ferrance, S. Swedberg, A. F. R. Hühmer, and J. P. Landers, "Polymerase chain reaction in polymeric Microchips:DNA amplification in less than 240 seconds," Anal. Biochem. **291**, 124-132 (2001).
16. R. P. Oda, M. A. Strausbauch, A. F. R. Huhmer, N. Borson, S. R. Jurrens, J. Craighead, P. J. Wettstein, B. Eckloff, B. Kline, and J. P. Landers, "Infrared-mediated thermocycling for ultrafast polymerase chain reaction amplification of DNA," Anal. Chem. **70**, 4361-4368 (1998).
17. M. He, J. S. Edgar, G. D. M. Jeffries, R. M. Lorenz, J. P. Shelby, and D. T. Chiu, "Selective encapsulation of single cells and subcellular organelles into picoliter- and femtoliter-volume droplets," Anal. Chem. **77**, 1539-1544 (2005).
18. M. He, C. Sun, and D. Chiu, "Concentrating solutes and nanoparticles within individual aqueous microdroplets," Anal. Chem. **76**, 1222-1227 (2004).
19. H. Terazono, A. Hattori, H. Takei, K. Takeda, and K. Yasuda, "Development of 1480nm photothermal high-speed real-time polymerase chain reaction system for rapid nucleotide recognition," Jpn. J. Appl. Phys. **47**, 5212-5216 (2008).
20. H. Kim, S. Vishniakou and G. W. Faris, "Petri dish PCR: Laser-heated reactions in nanoliter droplet arrays" Lab Chip (to be published).
21. L. Kou, D. Labrie, and P. Chylek, "Refractive indices of water and ice in the 0.65- to 2.5-μm spectral range," Appl. Opt. **32**, 3531-3540 (1993).
22. J. Coppeta and C. Rogers, "Dual emission laser induced fluorescence for direct planar scalar behavior measurements," Exp. Fluids **25**, 1-15 (1998).
23. D. Ross, M. Gaitan, and L. E. Locascio, "Temperature measurement in microfluidic systems using a temperature-dependent fluorescent dye," Anal. Chem. **73**, 4117-4123 (2001).
24. M. N. Slyadnev, Y. Tanaka, M. Tokeshi, and T. Kitamori, "Photothermal temperature control of a chemical reaction on a microchip using an infrared diode laser," Anal. Chem. **73**, 4037-4044 (2001).
25. B. Vogelstein and K. W. Kinzler, "Digital PCR," Proc. Natl. Acad. Sci. USA **96**, 9236-9241 (1999).
26. K. Bross and W. Krone, "On the number of ribosomal RNA genes in man," Human Genet. **14**, 137-141 (1972).
27. R. G. Worton, J. Sutherland, J. E. Sylvester, H. F. Willard, S. Bodrug, I. Dubé, C. Duff, V. Kean, P. N. Ray, and R. D. Schmickel, "Human ribosomal RNA genes: orientation of the tandem array and conservation of the 5' end," Science. **239**, 64-68. (1988).
28. P. H. Dear and P. R. Cook, "Cellular gels. Purifying and mapping long DNA molecules," Biochem J. **273**, 695-699. (1991).
29. B. C. Delidow, J. P. Lynch, J. J. Peluso, and B. A. White, "Polymerase chain reaction," in *Basic DNA and RNA Protocols*, A. Harwood, ed. (Humana Press, Totowa, NJ, 1996), pp. 275-292.
30. H. A. Druett, "Equilibrium temperature of a small sphere suspended in air and exposed to solar radiation," Nature **201**, 611 (1964).
31. S. Goodhew and R. Griffiths, "Analysis of thermal-probe measurements using an iterative method to give sample conductivity and diffusivity data," Applied Energy **77**, 205-223 (2004).
32. M. M. Kiss, L. Ortoleva-Donnelly, N. R. Beer, J. Warner, C. G. Bailey, B. W. Colston, J. M. Rothberg, D. R. Link, and J. H. Leamon, "High-Throughput Quantitative Polymerase Chain Reaction in Picoliter Droplets," Anal Chem **80**, 8975-8981 (2008).
33. J. Clausell-Tormos, D. Lieber, J. C. Baret, A. El-Harrak, O. J. Miller, L. Frenz, J. Blouwolff, K. J. Humphry, S. Köster, H. Duan, C. Holtze, D. A. Weitz, A. D. Griffiths, and C. A. Merten, "Droplet-based microfluidic platforms for the encapsulation and screening of mammalian cells and multicellular organisms," Chem. Biol. **15**, 427-437 (2008).
34. S. Köster, F. E. Angilè, H. Duan, J. J. Agrestil, A. Wintner, C. Schmitz, A. C. Rowat, C. A. Merten, D. Pisignano, A. D. Griffiths, and D. A. Weitz, "Drop-based microfluidic devices for encapsulation of single cells," Lab Chip **8**, 1110-1115 (2008).

1. Introduction

Recent advances in optical microfluidics have demonstrated the practical applications of how light can control a liquid sample in the same way as the fluidic circuitry [1-4]. With laser heating operating on a droplet, a convenient reaction chamber unit for miniaturized assay systems [5-7], many optical fluidic control blocks have been simulated. A laser has been used for manipulation and mixing of droplets [3, 4, 8] and a droplet valve, sorter, fuser, or divider [9]. Thus, light has proved to be an excellent method to mimic the classical microfluidic controller on a planar surface.

Many biochemical assays, however, require more than fluidic circuitry. For example, the polymerase chain reaction (PCR), one of the more prevalent biochemical assays, requires temperature cycling. One method commonly used for miniaturized high-throughput droplet-

#103676 - $15.00 USD Received 11 Nov 2008; revised 18 Dec 2008; accepted 20 Dec 2008; published 24 Dec 2008

based PCR chips [10-13] incorporates a heater and/or temperature sensor inside the substrate. This approach requires complex design and fabrication steps. Miniaturized contact heating methods can be impacted by limited throughput [12, 13] and cross contamination if the sample is in direct contact with the heater [14].

Infrared optical methods offer a simple non-contact heating method in which the heating source can be independent and remote from the PCR mixture. While infrared heating for PCR can be performed with conventional light sources [15, 16], a laser heating method can provide higher intensities and better power and wavelength control. Moreover, the same infrared laser that we used previously for droplet movement and mixing [3, 8] can also be used to drive the heating cycles of PCR on the same platform. Another complementary advantage of the droplet approach is that the size of the droplet is easily matched to the short extinction length of the infrared laser in water, thus naturally following the trend of miniaturization while also optimizing efficiency. Droplets as water-in-oil emulsions are indeed one of the most attractive candidates for microfluidic reactors in the application of lab-on-a-chip methods for high-throughput assays [5-7] because they are stable and can be easily generated and spatially arrayed on a solid substrate without crosstalk between neighboring droplets [17, 18].

We show how a low-power (~30 mW) infrared laser can drive temperature cycling for PCR by rapidly switching the laser on and off as illustrated in Fig. 1(a). The reaction chambers are nanoliter droplets as water-in-oil emulsions on a disposable plastic substrate. Recently, Terazono et al. reported a similar heating scheme using a laser power as high as 1 W for nanodroplets that have comparable volumes to ours [19]. In our work, we show that with careful choice of the substrate we can use at least 30 times less laser power, which is indeed close to the minimally required power to heat a droplet of this size for PCR. The importance of the low power consumption cannot be exaggerated in the application of PCR because highly parallel reactions are the standard of current PCR technology. The optical heating method seems to be one of the promising candidates for dramatic improvement of the scalability of this technology.

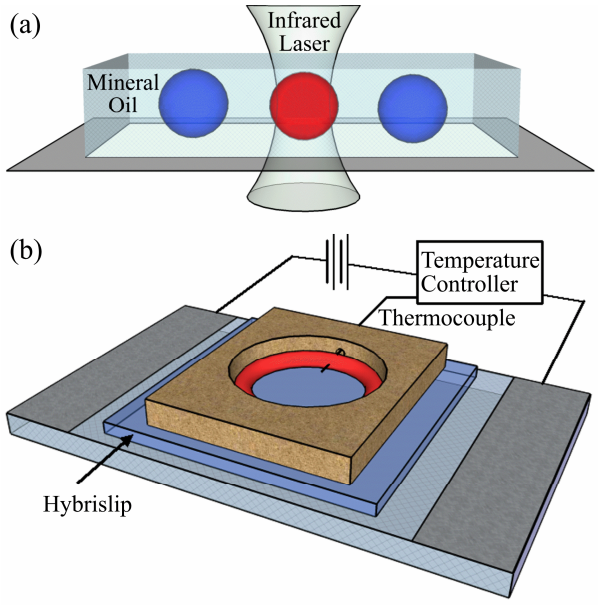

Fig 1. (a) Illustration of laser-irradiated droplets dispersed in mineral oil for PCR on a microscope stage. (b) Home-built PCR chamber that holds the mineral oil and droplets at a constant temperature based on a conductive glass slide. The silicon O-ring forces the top surface of the oil to be optically flat, and a single-use hydrophobic Hybrislip is inserted as the floor of the chamber.

#103676 - $15.00 USD Received 11 Nov 2008; revised 18 Dec 2008; accepted 20 Dec 2008; published 24 Dec 2008

2. Materials and methods

2.1 PCR sample preparation

As suggested by the assay manufacturer and other work in our laboratory [20], the PCR mixture was prepared in 20 μl volumes that contain 10 μl of Taqman Fast Universal PCR Master Mix 2X (#4352042, Applied Biosystems), 1 μl of Taqman gene expression assay of primer/probe set targeting the eukaryotic 18S rRNA gene (#4331182, Applied Biosystems), and human genomic DNA (#4312660, Applied Biosystems) diluted in 9 μl of DI water. The raw concentration of the template DNA was 10 ng/μl. In some cases, LDS 698 was dissolved at a final concentration of 0.01 mM as a temperature marker. The length of amplicon was 187 base pairs (bp).

2.2 Fluorescence microscopy

An inverted Nikon microscope with dual fluorescence filter cube turrets (TE2000, Nikon) provides the base of the optical setup, with the top filter cube for fluorescence collection and the bottom one for delivery of the infrared laser beam for heating the droplet. A set of band-pass filters was used for fluorescence detection with 480/40 nm for excitation, 520/40 nm for emission of FAM, and 695/100 nm for emission of LDS 698. A 530 nm long-pass filter was also inserted in the optical emission path to cut off any remaining excitation light. Images were acquired with a cooled CCD camera (Retiga Exi, Qimaging).

2.3 PCR setup

A reaction chamber that can hold the temperature to within ±0.2°C was built based on a conductive glass slide (indium tin oxide coated glass, Nanocs) with a temperature controller (CN96111TR-C2, Omega) as shown in Fig. 1 (b). A cylindrical well 6 mm in height and 20 mm in diameter machined in a plastic substrate was placed on top of a Hybrislip (HS22, Grace Bio-labs), which in turn rested on the conductive glass slide. (The Hybrislip, a single-use hydrophobic cover that replaces the cover slip, is a 0.25-mm-thick square plastic piece made of polycarbonate for rigidity and temperature resistance.) A silicon O-ring was inserted, forming the wall of the chamber to keep the oil phase optically flat by geometrically forcing a smooth interface between the O-ring and the oil phase. A thin thermocouple was fixed in contact with the chamber floor to measure the temperature of the substrate. Two edges of the conductive glass slide were electrically connected to a dc power supply that was regulated by the temperature controller through the feedback from the thermocouple. After mineral oil (M5310, Sigma) was deposited in the chamber, PCR mixture droplets were dispensed by a micropipette into the oil phase to form 20- to 100-nl droplets. A single dispensing action often produced multiple droplets, each with a volume smaller than the minimum dispensing volume (~100 nl) of the pipette.

2.4 PCR reaction

For the PCR heating cycle, a defocused infrared diode laser at a wavelength of 1.46 μm (Furukawa Electric) was aimed at a single droplet. This wavelength was chosen because water has a strong vibrational absorption band with an extinction coefficient as high as 32.4 cm^{-1} [21] while the mineral oil has about 40 times less absorption at this wavelength according to our measurement (not shown). A low noise current source (LDX-3620, ILX Lightwave) supplied the laser power. The current was in turn controlled by a computer. The laser was defocused at the object plane so that the droplet could be heated uniformly. The beam size was about 200 μm at FWHM using a 10x objective lens. The maximum laser power after the objective lens was 70 mW. The laser power needed to be adjusted to maintain similar temperatures for droplets with different sizes. Temperature monitoring was performed by measuring the fluorescence intensity of a temperature-sensitive dye. LDS 698 is known to be

#103676 - $15.00 USD Received 11 Nov 2008; revised 18 Dec 2008; accepted 20 Dec 2008; published 24 Dec 2008

temperature sensitive [22] and has a fluorescence spectrum far in the red, so it does not interfere with either FAM, a probe dye with a ~520 nm emission peak, or ROX, a calibration dye with a ~610 nm emission peak that is pre-mixed in the PCR master mix.

We slightly modified the proposed protocol from Applied Biosystems and found optimized conditions of 40 cycles of 2 seconds at 93°C for melting and 8 seconds at 58°C for annealing/extension, in addition to the initial enzyme activation at 93°C for 10 seconds. This is comparable to the protocol used by Neuzil at al. [13]. The laser heating was used only for melting the double-stranded DNA and initial enzyme activation, while the temperature of the chamber was set at 58°C for the annealing/extension steps. To drive the heating cycles of droplets with diameters of ~400 μm, we typically used 30 mW of laser power.

Bright field images were taken before and after the PCR reaction to make sure that the volume or concentration was not changing significantly during the reaction. Image acquisition and laser power control were fully automated by Labview software.

A commercial real-time PCR machine (7500, Applied Biosystems) was used for comparison with the amplification efficiency of the laser-assisted PCR.

2.5 Data analysis

The fluorescence images acquired at each cycle were processed by averaging only nonzero intensity pixels (i.e., the droplet and not the surrounding oil). A simple computer code was written to determine the cycle of threshold (C_t) when the increase of the averaged fluorescence intensity surpassed the standard deviation computed from all the previous cycles (the baseline standard deviation). For this work, we required the fluorescence intensity to exceed the baseline standard deviation and grow by at least one baseline standard deviation for three successive cycles. This avoids selecting a C_t value based on statistical fluctuations. Once this condition was met, a linear fit was performed between the intensity of the first of these three cycles and the intensity of the previous cycle. The fractional C_t was then determined as the point where this linear fit crossed the baseline standard deviation. The same algorithm was applied to determine C_t of the commercial PCR system with the component data from FAM fluorescence.

3. Results and discussion

3.1 Temperature dependence of LDS 698

For successful PCR reactions and further application to quantitative parallel assays, it is critical to measure and regulate the temperature of each reaction droplet accurately during the heating cycle to ensure the same amplification efficiency over all the reaction droplets. To measure the temperature of a droplet with volume in the nanoliter range and a temperature significantly different from that of the ambient oil phase, a non-contact temperature measurement technique was employed using a temperature-sensitive fluorescent dye. Among several dyes that have been reported to be applicable for this purpose [22-24], LDS 698 turned out to be most suitable for our application because it is highly hydrophilic, it has a far-red fluorescence spectrum, and moderate but detectable intensity changes over the large temperature range for PCR.

#103676 - $15.00 USD Received 11 Nov 2008; revised 18 Dec 2008; accepted 20 Dec 2008; published 24 Dec 2008

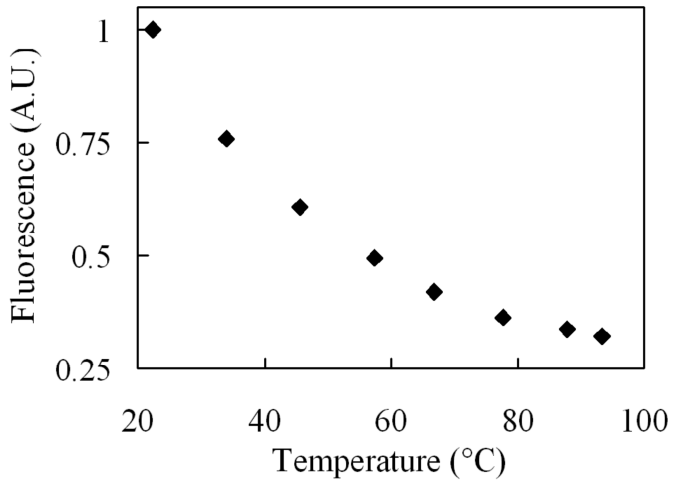

Fig 2. Normalized fluorescence intensity of LDS 698 dissolved in the aqueous droplet as a function of temperature.

LDS 698 was diluted to a final concentration of 0.01 mM at the pH of the PCR buffer and its fluorescence intensity was monitored in the temperature range necessary for the PCR reaction. We found a monotonically decreasing intensity response as the temperature increased, as presented in Fig. 2. The intensity ratio between the annealing (~58°C) and melting (~93°C) temperatures was measured to be 0.65 on average. This ratio was used for adjustment of the laser power for PCR in the droplets in oil maintained at the annealing/extension temperature.

We chose a laser with a wavelength used in the telecommunication industry. In addition to the low cost of the laser, the wavelength of 1.46 μm is also very beneficial to our application because it corresponds with a strong absorption band in water. The 1/e absorption length for water at this wavelength is ~300 μm, which is quite close to the droplet size, leading to efficient absorption. Because of the small droplet size, heating is very rapid, allowing very short heating cycles with this laser.

3.2 Laser heating PCR from annealing/extension temperature

The laser power was adjusted to heat the droplets to the melting temperature while the reaction chamber was maintained at 58°C. We collected images of FAM fluorescence in the droplet following the end of each extension heating period. When using Taqman probes in real-time PCR, each cycle of amplification cleaves fluorescent dye molecules (FAM in our case) from a quenching partner, so that the FAM fluorescence intensity indicates the degree of amplification of the target DNA. A plot of FAM fluorescence versus heating cycle number follows a profile typical for a real-time PCR amplification curve (i.e., flat, exponential, linear, exponential, flat). With droplets at a target DNA concentration of 4 ng/μl, the FAM fluorescence intensity rose above the background after around 17 heating cycles with laser heating as seen in Fig. 3 and Fig. 4. Amplification curves in Fig. 3 were drawn by averaging the intensity over the fluorescence images acquired at each cycle as shown in Fig. 4.

#103676 - $15.00 USD Received 11 Nov 2008; revised 18 Dec 2008; accepted 20 Dec 2008; published 24 Dec 2008

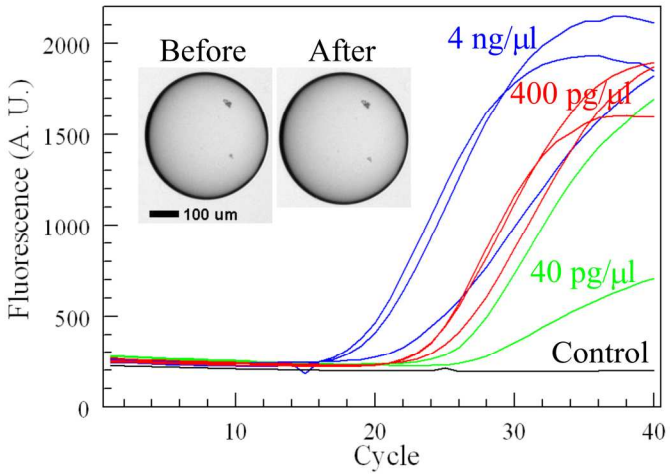

Fig 3. Amplification curves of droplet-based PCR with laser heating at four concentrations. The 4 ng/µl, 400 pg/µl, 40 pg/µl concentrations correspond to roughly 14,000, 1,400, and 140 target copies per droplet, respectively. Bright field images of a PCR mixture droplet dispersed in the mineral oil phase before and after PCR with a 100 µm scale bar are also shown as insets.

To test the quantitative capability of the laser heating PCR assay, droplets with three different concentrations of target DNA were prepared. With prior calibration of the laser power, droplets were successfully amplified in most cases. Ten-fold sequential dilution of the target DNA in the PCR mixture generated C_t's (cycle of threshold, when the fluorescence intensity exceeds the background level) determined to be 16.6 ± 0.95, 21.8 ± 1.1 and 25.8 ± 2.7, respectively, for droplets with 4 ng/µl, 400 pg/µl, and 40 pg/µl target concentrations. Typical amplification curves collected for each concentration are shown in Fig. 3. With 100% amplification efficiency, the C_t is expected to increase by 3.3 with every 10-fold dilution of the target concentration. According to our data, the increase in C_t with dilution was rather higher than this, which might be due to several causes as discussed below. The bright field images of a 4 ng/µl droplet before and after amplification, shown as an inset in Fig. 3, show that the size or volume did not change significantly during the laser heating PCR reaction.

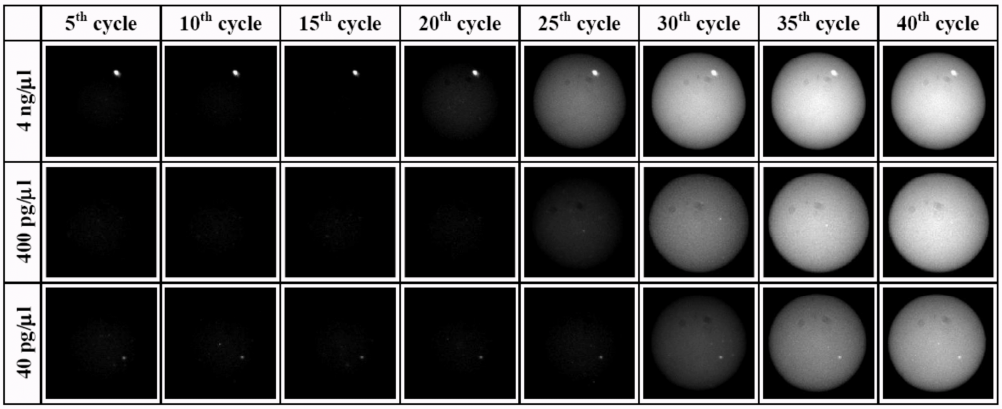

Fig 4. Fluorescence images from FAM emission of droplets during the amplification cycle of laser heating PCR with the oil phase held at 58°C.

#103676 - $15.00 USD Received 11 Nov 2008; revised 18 Dec 2008; accepted 20 Dec 2008; published 24 Dec 2008

We performed a regular 96-well reaction plate real-time PCR with a commercial instrument to validate our droplet-based PCR results. A C_t of 16.9 was determined in case of the conventional PCR with a 2 ng/μl concentration, which suggests that C_t of 15.9 is expected for the twice-concentrated 4 ng/μl PCR mixture we used with the laser heating. Even though the observed C_t value of 16.6 is slightly higher than expected, it is reasonably close within the variation of our data and indicates that our amplification efficiency is close to that of a commercial instrument. This is notable because the commercial system uses a volume of 10 μl, which is at least 300 times larger than the volumes we use. In other words, we achieve C_t values similar to those of the commercial instrument in spite of having roughly 300 times fewer target copies in our sample.

A careful analysis of the amplification curves in Fig. 3 shows that the baseline is not flat but sloped downward, which may have affected the determination of C_t for the droplet-based PCR. While we believe that the simultaneous monitoring of a calibration dye such as ROX will help to fix this issue as in a conventional Taqman assay, it was experimentally concluded that this decrease was not caused by the simple photobleaching of FAM. A control experiment without the heating laser did not cause as significant a decrease in the fluorescence intensity as did the laser heating. It appears unlikely that the heating is increasing photobleaching through increased kinetic rates because the heater and fluorescence illumination are used sequentially, not simultaneously. In addition, it is quite unlikely that the laser could cause photobleaching due to the long wavelength (1.46 μm). The source of the downward-sloping baseline is not currently understood. The downward slope is extremely small compared to the rise during the exponential phase of the PCR response, so the impact on the results is extremely small. It is noteworthy that photobleaching of FAM should be negligible as long as the fluorophores are strongly quenched as Taqman probes.

Since we are using small reaction volumes, attention should be paid to the number of target templates contained in a single droplet. With a typical droplet volume of 30 nl in our experiment and the mass of a single copy of human genome at ~3 pg [25], the 4 ng/μl droplet is estimated to have about 40 copies of genome, while the 100-times-diluted 40 pg/μl droplet will have only 0.4 haploid genome copies on average. However, there are 300-400 copies of the genes encoding 18S ribosomal RNA occurring in five pairs of chromosomes in each human genome [26, 27]. Furthermore, pipetting can readily produce hydrodynamic shearing of DNA longer than approximately 100,000 base pairs [28], facilitating distribution of the 18S gene during dilution. Thus, the 40 pg/μl droplets still contain 120-160 copies of target templates, and it is not surprising that all the droplets containing only 0.4 copies of human genome were successfully amplified.

The shortest total reaction time for 40 cycles of PCR without significantly compromising the C_t was 370 seconds with 10, 2, and 7 seconds for the enzyme activation, melting, and annealing/extension steps, respectively. With laser heating of nanodroplets, the time scales for heating and cooling are negligible compared with the periods for melting and annealing/extension. Thus the most time-consuming step of the laser heating PCR is the extension step, when the enzyme adds bases between the primers, which consumes most of the 7 seconds for annealing and extension. In comparison, the shortest annealing/extension time documented for a contact-heater-based real-time PCR was 6.5 seconds for a 82 bp amplicon length by Neuzil et al. [13]. Our results compare favorably with Neuzil since our annealing/extension time is almost identical to theirs and our 187 bp amplicon was more than twice as long. The polymerase extension speed is 30-60 bases per second [29], which agrees well with our results, which require an extension rate of more than 27 bases per second, depending on the time required for annealing. By virtually eliminating the time required for heat transfer, the PCR reaction is limited only by biochemical reaction rates. The extremely fast heat transfer explains why our extension time is quite close to that of Neuzil's in spite of the amplicon being twice as long.

#103676 - $15.00 USD Received 11 Nov 2008; revised 18 Dec 2008; accepted 20 Dec 2008; published 24 Dec 2008

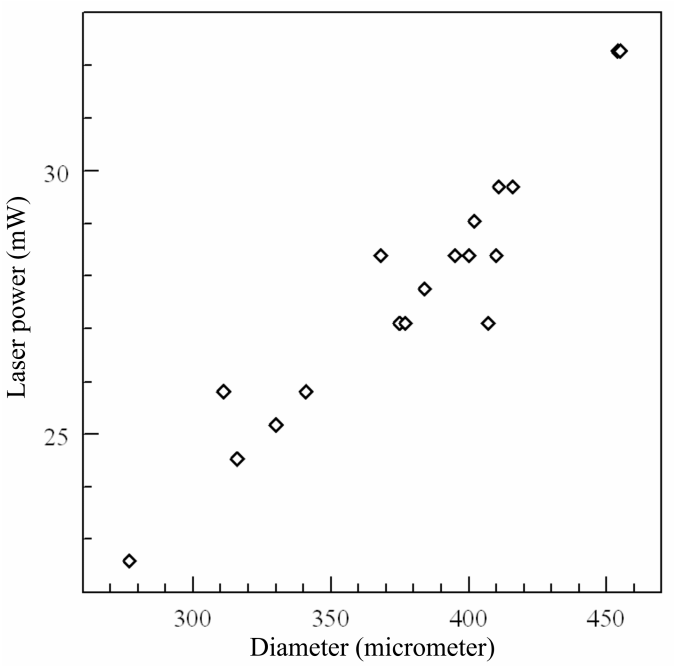

Fig. 5 Laser power required for the successful PCR amplification as a function of droplet diameter.

A plot of the laser power required for successful PCR amplification for different droplet sizes is shown in Fig. 5. The plot shows that the power grows linearly with the droplet size as expected (see next paragraph). In cases where droplet diameter is not well controlled, the laser power should be varied proportionally to the droplet diameter similarly to Fig. 5 to obtain the most reliable results. However a better approach is to prepare monodisperse droplets.

The heat loss from the droplet is dominated by the conductive heat loss to the lower-temperature oil phase. In the case of a perfect sphere in a heated reservoir at a temperature T_0, the heat flow required to keep the sphere at a higher temperature at T_1 with only conductive heat loss, is given as [30],

$$Q = 4\pi \cdot k \cdot r \cdot (T_1 - T_0) \quad (1)$$

where k and r are thermal conductivity of the reservoir and radius of the sphere, respectively. With k ~ 0.15 $Wm^{-1}K^{-1}$ for mineral oil [31] and a typical radius r of 200 μm for droplets tested in this work, Eq. (1) yields a minimum power of 13 mW to keep a spherical droplet at 95°C dispersed in the mineral oil at 60°C. On the other hand, the radiation heat loss is negligible with ~160 μW heat loss for the same conditions. The typical laser power used for the heating cycles of PCR was 30 mW for a droplet with a diameter of 400 μm. Considering that only a portion of the laser is absorbed by the droplet (the droplet diameter is at most slightly larger than the 1/e absorption length at the longest optical pathlength through the center of the droplet, and less near the edges), 30 mW is reasonably close to the minimum power required for optical heating of droplets in this size range. In case of the work by Terazono et al. [19], the significantly higher power requirement of ~1 W for the same droplet volume seems to be due to a more flattened droplet profile on a hydrophilic glass substrate, resulting in a shorter absorption length.

We showed that low power (~30 mW) laser heating, if combined with a droplet-based PCR system, has significant advantages compared with other PCR heating methods including (1) extremely fast heating and cooling due to the selective and direct heating of the PCR buffer and not the oil; (2) no need for the fluidic circuitry or microheaters on the disposable reaction substrate; (3) straightforward selection of droplets for amplification; (4) a very small

#103676 - $15.00 USD Received 11 Nov 2008; revised 18 Dec 2008; accepted 20 Dec 2008; published 24 Dec 2008

reaction volume; and (5) amplification of single droplets without influencing neighboring droplets.

In the current work, we amplified a single droplet at a time mainly because the power of our laser is enough to sustain amplification in a single droplet with 20-40 nl droplets, which is about 300 times less than the volume required for the conventional tube-based PCR assay. We are currently developing spotting techniques that can produce a large number of droplets in a regularly spaced array so that multiple droplets can be assayed at the same time with a more powerful laser. Therefore, this technology can be adapted to a highly parallel array-based PCR method with all-optical control and readout. Possible applications include digital PCR for the accurate quantification of targets [25, 32] and an assay for nucleic acids in cell arrays encapsulated in droplets [33, 34].

Acknowledgments

This research is supported by the National Cancer Institute under Grant CA118526.

#103676 - $15.00 USD Received 11 Nov 2008; revised 18 Dec 2008; accepted 20 Dec 2008; published 24 Dec 2008